Efficient Non-doped Near Infrared Organic Light-Emitting Devices Based on Fluorophores with Aggregation-Induced Emission Enhancement

ARTICLE *in* CHEMISTRY OF MATERIALS · MAY 2012

Impact Factor: 8.35 · DOI: 10.1021/cm3008733

5 AUTHORS, INCLUDING:

Ji Qi
Chinese Academy of Sciences
16 PUBLICATIONS **177** CITATIONS

SEE PROFILE

Zhi Yuan Wang
Carleton University
196 PUBLICATIONS **3,245** CITATIONS

SEE PROFILE

CHEMISTRY OF MATERIALS

Article

pubs.acs.org/cm

Efficient Non-doped Near Infrared Organic Light-Emitting Devices Based on Fluorophores with Aggregation-Induced Emission Enhancement

Xiaobo Du,[†,§] Ji Qi,[†,§] Zhiqiang Zhang,[†] Dongge Ma,[†] and Zhi Y. Wang*[,†,‡]

[†]State Key Laboratory of Polymer Physics and Chemistry, Changchun Institute of Applied Chemistry, Chinese Academy of Sciences, Changchun 130022, P.R. China

[‡]Department of Chemistry, Carleton University, 1125 Colonel By Drive, Ottawa, Ontario K1S 5B6, Canada

[§]Graduate School of Chinese Academy of Sciences, Beijing 100039, P.R. China

Supporting Information

ABSTRACT: A family of donor−acceptor−donor (D−A−D) type near-infrared (NIR) fluorophores containing rigid nonplanar conjugated tetraphenylethene (TPE) moieties was designed and synthesized through Stille coupling reactions with electron-deficient [1,2,5]thiadiazolo[3,4-g]quinoxaline (QTD) or benzo[1,2-c;4,5-c′]bis[1,2,5]thiadiazole (BBTD) as acceptors. The absorption, fluorescence, and electrochemical properties were studied. These compounds exhibited good aggregation-induced emission enhancement (AIEE) property, as a result of the twisted TPE units, which restrict the intramolecular rotation and reduce the $\pi-\pi$ stacking. Photoluminescence of these chromophores ranges from 600 to 1100 nm, and their HOMO−LUMO gaps are between 1.85 and 1.50 eV. Non-doped organic light-emitting diodes (OLEDs) based on these fluorophores were made and exhibited EL emission spectra peaking from 706 to 864 nm. The external quantum efficiency (EQE) of these devices ranged from 0.89% to 0.20% and remained fairly constant over a range of current density of 100−300 mA cm^{-2}. The device with the highest solid fluorescence efficiency emitter **1a** shows the best performance with a maximum radiance of 2917 mW Sr^{-1} m^{-2} and EQE of 0.89%. A contrast between nondoped and doped OLEDs with these materials confirms that AIEE compounds are suitable for fabricate efficient nondoped NIR OLEDs.

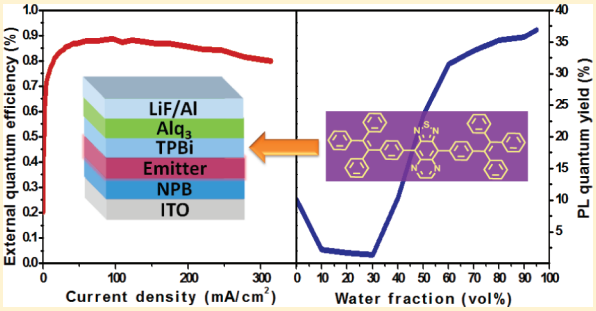

KEYWORDS: *near infrared, AIEE, OLEDs, donor−acceptor*

INTRODUCTION

Near-infrared (NIR) fluorescent materials are fundamentally interesting and practically useful as NIR fluorescent tags for bioimaging[1−3] and chemosensing[4] or as NIR organic light-emitting diodes (OLEDs).[5,6] For biological applications, NIR fluorophores with the emission wavelength between 650 and 1200 nm are more highly desirable than visible fluorescence probes, because of a better spectral separation from autofluorescence and low light scattering in biological tissues.[7] For potential applications in optical communication,[8] night-vision displays[9] and information-secured display,[10] highly efficient NIR fluorophores are urgently needed for use in OLEDs.

However, many known fluorophores exhibit high fluorescence in dilute solutions but weak or no emission in the solid state because of aggregation-caused emission quenching (ACEQ).[11−14] The ACEQ is generally attributed to a nonradiative deactivation process, such as excitonic coupling, excimer formation, and excitation energy migration to the impurity traps.[15,16] Most of the NIR organic fluorophores are donor−acceptor type or flat π-conjugated molecules and, thus, are more prone to molecular aggregation and fluorescence quenching in the solid state.[17−19] In addition, NIR fluorophores with low band gaps often have more vibronic coupling between ground and excited state, which promotes the nonradiative deactivation pathways.[20] Therefore, most NIR-absorbing chromophores show no or low fluorescence in the solid state and could only be used as a dopant in NIR OLEDs.[21−23] An effective approach is to employ phosphorescent sensitized fluorescence by codoped with phosphorescent dye,[24,25] which has been proved useful in improving the device efficiencies of fluorescent NIR OLEDs to the levels of phosphorescent NIR OLEDs.[26−28] However, efficacious doping often requires precise control of doping concentration, and the bimolecular interactions emission quenching at high exciton densities cause a rapid decrease in quantum efficiency for high currents or high doping concentrations.[29] The non-doped OLEDs with the emission above 700 nm still show a low external quantum

Received: March 20, 2012
Revised: May 21, 2012
Published: May 22, 2012

   dx.doi.org/10.1021/cm3008733 | *Chem. Mater.* 2012, 24, 2178−2185

Scheme 1. Synthetic Route to Compounds 1a,b and 2a,b

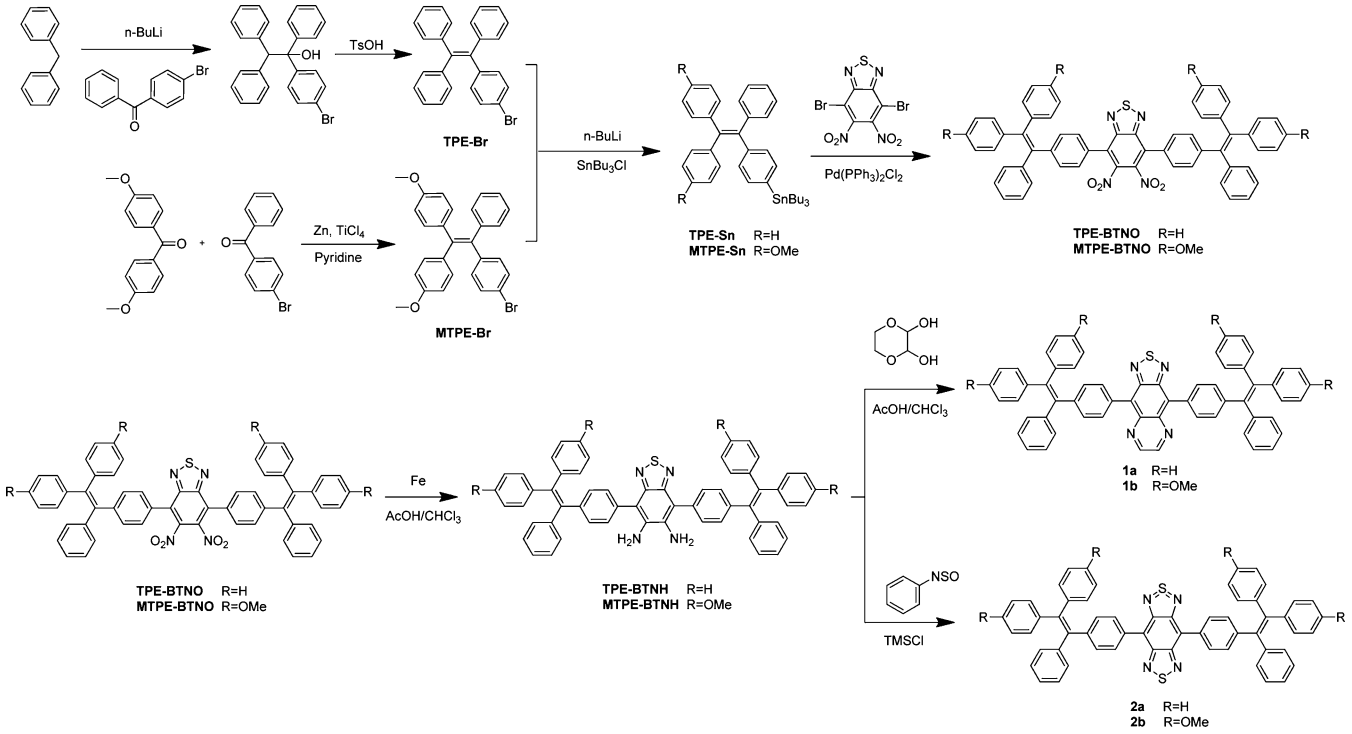

efficiency (EQE) and are not suitable for practical applications.[30−33]

A molecular approach to overcoming the ACEQ in organic fluorophores was initiated by Tang in 2001, which involves the introduction of a propeller-like group to reduce or eliminate the $\pi-\pi$ stacking and molecular rotational motions in the solid state.[34] Consequently, a variety of compounds such as distyrylbenzene, fluorene, pentacene, and pyrene derivatives are enabled to display the aggregation-induced emission enhancement (AIEE) and show a higher fluorescence efficiency in the solid state than in solution.[35−38] However, realization of the AIEE in NIR fluorophores has yet to be demonstrated.

A twisted tetraphenylethene (TPE) has the excellent AIEE property and has also been shown to be a unique AIEE enabling unit for many organic chromophores.[39,40] Incorporation of TPE units into the chemical structures of poor fluorophores could significantly improve their fluorescence efficiency in the solid state.[41] Accordingly, we envision that by introduction of the TPE units in a low band gap chromophore such as a π-conjugated donor−acceptor (D−A) system,[42,43] the AIEE in the NIR spectral region can be realized. By design, the TPE group should be a part of the conjugated moiety to prevent the $\pi-\pi$ stacking and enable the AIEE property of the designed compounds and also act as an electron donor with an option of further substitution with additional electron-donating groups. Guided by this design principle, we report the synthesis of the D−A−D type NIR fluorescent compounds with the AIEE property and non-doped NIR OLEDs with a single emission peak centered above 700 nm and up to 1000 nm. These devices are stable and show very little efficiency roll-off at high current densities. The device performance is considered to be the best for non-doped NIR OLEDs reported to date.

EXPERIMENTAL SECTION

General Information. Synthetic routes of these fluorescent compounds are described in Scheme 1. All chemicals and reagents were used as received from commercial sources. 4,7-Dibromo-5,6-dinitro-2,1,3-benzothiadiazole[44] and 1-(4-bromophenyl)-1,2,2-triphenylethylene (TPE-Br)[45] were prepared according to literature methods.

^{1}H NMR (300 MHz) spectra of all the samples in $CDCl_3$ were recorded on a Bruker Avance NMR spectrometer. The high-temperature ^{13}C NMR data were obtained on a Varian Unity-400 MHz spectrometer at 393 K. Elemental analysis was performed on a Vario EL elemental analysis instrument. Matrix-assisted laser desorption ionization time-of-flight mass spectrometry (MALDI-TOF-MS) was performed on a Bruker Daltonics Autoflex III TOF/TOF. High-resolution mass spectrometry (HRMS) was obtained using a 7.0 T actively shielded Fourier transform ion cyclotron resonance mass spectrometer. The UV−vis−NIR absorption spectra were recorded on a Shimadzu UV-3600 spectrophotometer. Cyclic voltammetry was performed on a CHI660b electrochemical workstation, in dry dichloromethane containing *n*-Bu_4NPF_6 (0.1 M) with a scan rate of 50 mV/s at room temperature under argon, using a Pt disk (2 mm diameter) as the working electrode, a Pt wire as the counter electrode, and a Ag/AgCl electrode as a reference. The redox potentials were calibrated by using ferrocene as an internal standard. Thermogravimetric analysis (TGA) was performed on a PerkinElmer Thermal Analysis Instruments Pyris Diamond TG instrument from 50 to 600 °C at a heating rate of 10 °C/min under a continuous nitrogen flow.

The OLED was fabricated by thermal vacuum deposition on prepatterned ITO-coated glass substrates with sheet resistances of 10 Ω/square. The substrate was ultrasonically cleaned with acetone, detergent, deionized water, and ethanol in sequence, followed by oxygen-plasma cleaning. The thermal evaporation of organic materials was carried out at a chamber pressure of 10^{-4} Pa. The thickness of each layer was determined by a quartz thickness monitor. The effective size of the light-emitting diode was 16 mm^2. Current−voltage−power measurements were performed simultaneously using a Keithley 2400 source meter and a Newport 1830-C optical meter equipped with a Newport 818-UV silicon photodiode, respectively. The NIR photo-

dx.doi.org/10.1021/cm3008733 | Chem. Mater. 2012, 24, 2178−2185

luminescence (PL) and electroluminescence (EL) spectra were measured using a PTI fluorescence spectrophotometer with InGaAs detector. The visible EL was measured using a PR650 spectroscan photometer. The fluorescence quantum yield in THF solutions was estimated using IR-125 (Φ_F = 0.13 in DMSO)[50] as standards. All the measurements were carried out under ambient atmosphere at room temperature. The EQE of the NIR EL was determined according to the literature method, by measuring the light intensity in the forward direction and assuming the external emission profile to be Lambertian.[32,47]

Synthesis. *1-(4-Bromophenyl)-2,2-bis(4-methoxyphenyl)-1-phenylethene (MTPE-Br).* Bis(4-methoxyphenyl)methanone (9.73 g, 40.0 mmol), 4-bromo-benzophenone (12.54 g, 48.0 mmol), and Zn powder (13 g, 200 mmol) in dried THF (500 mL) were stirred at 0 °C under an argon atmosphere; then, $TiCl_4$ (17.6 mL, 160 mmol) was dropped into the reaction mixture with rapid stirring over 30 min. The mixture was heated to 80 °C for 24 h. After being cooled to room temperature, the reaction was quenched by the addition of 250 mL 10% aq K_2CO_3; the mixture was filtered to remove insoluble materials and washed with CH_2Cl_2. The organic layer was dried with anhydrous $MgSO_4$ and filtered. The solution was evaporated. The crude product was purified by column chromatography (PE/DCM = 1:1) to give 9.62 g (20.4 mmol) of MTPE-Br as a light yellow solid in 51% yield. ^{1}H NMR (300 MHz, $CDCl_3$) δ (ppm): 7.22 (d, 2H, J = 8.4 Hz), 7.12−7.08 (m, 3H), 7.01−6.98 (m, 2H), 6.95−6.87 (m, 6H), 6.68−6.61 (m, 4H), 3.75 (d, 6H, J = 8.4 Hz).

4,7-Bis[4-(1,2,2-triphenylvinyl)phenyl]-5,6-dinitrobenzo-2,1,3-thiadiazole (TPE-BTNO). TPE-Br (8.23 g, 20.0 mmol) in dried THF (150 mL) was stirred at −78 °C under an argon atmosphere, then *n*-BuLi (2.5 M in hexane, 12.0 mL, 30.0 mmol) was dropped into it over 20 min. After the mixture was stirred for 2 h, tributylstannyl chloride (10.1 mL, 36.0 mmol) was added to it and reacted for 12 h at 25 °C. The mixture was poured into water and extracted with ethyl acetate. Upon evaporation of the solvent, the crude product, 4,7-dibromo-5,6-dinitro-2,1,3-benzothiadiazole (3.07 g, 8.00 mmol), and $PdCl_2(PPh_3)_2$ (100 mg) in dried THF (150 mL) were stirred at 80 °C for 24 h under an argon atmosphere. After being cooled to the room temperature, the mixture was diluted with dichloromethane and washed with 100 mL saturated aqueous potassium fluoride solution and brine. The crude product was purified by column chromatography (PE/DCM = 1:2) to give compound TPE-BTNO as an orange solid (6.72 g, 95%). ^{1}H NMR (300 MHz, $CDCl_3$) δ (ppm): 7.30−7.27 (m, 4H), 7.21−7.02 (m, 34H). Anal. calcd for $C_{58}H_{38}N_4O_4S$: C, 78.54; H, 4.32; N, 6.32. Found: C, 77.91; H, 4.58; N, 6.12. MALDI-TOF-MS: m/z 886.3 (M^+).

4,7-Bis{4-[2,2-bis(4-methoxyphenyl)-1-phenylvinyl]phenyl}-5,6-dinitrobenzo-2,1,3-thiadiazole (MTPE-BTNO). Following the procedure for the preparation of TPE-BTNO, MTPE-BTNO was obtained as a purple solid (7.58 g, 94%). ^{1}H NMR (300 MHz, $CDCl_3$) δ (ppm): 7.30−7.25 (m, 4H), 7.19−7.12 (m, 14H), 7.00−6.93 (m, 8H), 6.71−6.64 (m, 8H), 3.76 (d, 12H, J = 5.7 Hz). Anal. calcd for $C_{62}H_{46}N_4O_8S$: C, 73.94; H, 4.60; N, 5.56. Found: C, 73.40; H, 4.63; N, 5.32. MALDI-TOF-MS: m/z 1006.3 (M^+).

4,7-Bis[4-(1,2,2-triphenylvinyl)phenyl]-5,6-diaminobenzo-2,1,3-thiadiazole (TPE-BTNH). TPE-BTNO (4.44 g, 5.00 mmol) and iron dust (3.35 g, 60.0 mmol) in acetic acid (180 mL) and $CHCl_3$ (180 mL) was stirred at 80 °C for 36 h under an argon atmosphere. After being cooled to the room temperature, the mixture was poured into water, and the resulting solids were collected by filtration. The mixture was dissolved in chloroform and was filtered to remove insoluble materials. Upon evaporation of the filtrate, the crude product was recrystallized by chloroform to afford the product as light yellow solid (2.65 g, 64%). ^{1}H NMR (300 MHz, $CDCl_3$) δ (ppm): 7.32 (d, 4H, J = 8.4 Hz), 7.22 (d, 4H, J = 8.4 Hz), 7.14−7.04 (m, 30H), 3.87 (s, 4H).

4,7-Bis{4-[2,2-bis(4-methoxyphenyl)-1-phenylvinyl]phenyl}-5,6-diaminobenzo-2,1,3-thiadiazole (MTPE-BTNH). MTPE-BTNH was synthesized according to the same procedure as that used in the preparation of TPE-BTNH to obtain a yellow solid at 59% yield. ^{1}H NMR (300 MHz, $CDCl_3$) δ (ppm): 7.33 (d, 4H, J = 8.4 Hz), 7.21 (d, 4H, J = 8.1 Hz), 7.14 (s, 10H), 7.03−6.96 (m, 8H), 6.69−6.64 (m, 8H), 3.75 (s, 16H).

*4,9-Bis[4-(1,2,2-triphenylvinyl)phenyl][1,2,5]thiadiazolo-[3,4-g]-quinoxaline (**1a**).* TPE-BTNH (0.414 g, 0.50 mmol) and 1,4-dioxane-2,3-diol (0.120 g, 1.00 mmol) in acetic acid (30 mL) and $CHCl_3$ (30 mL) were stirred at 30 °C for 6 h under an argon atmosphere. After being cooled to the room temperature, the mixture was poured into water and the resulting solids were collected by filtration. The crude product was purified by column chromatography (PE/DCM = 1:3) to give compound **1a** as a red solid (0.297 g, 70%). ^{1}H NMR (300 MHz, $CDCl_3$) δ (ppm): 8.82 (s, 2H), 7.64(d, 4H, J = 8.4 Hz), 7.27−7.24 (m, 4H), 7.19−7.07 (m, 30H). ^{13}C NMR (100 MHz, $C_2D_2Cl_4$, 393K) δ (ppm): 154.07, 146.34, 144.84, 144.70, 144.36, 142.93, 142.10, 139.31, 134.13, 133.11, 132.32, 132.24, 132.17, 131.18, 128.68, 128.55, 127.37, 127.28. HRMS (ESI, m/z): $(M+H)^+$ calcd for $C_{60}H_{40}N_4S$, 849.30518; found, 849.30487.

*4,9-Bis{4-[2,2-bis(4-methoxyphenyl)-1-phenylvinyl]phenyl}[1,2,5]thiadiazolo-[3,4-g]quinoxaline (**1b**).* MTPE-BTNH (0.474 g, 0.50 mmol) and 1,4-dioxane-2,3-diol (0.120 g, 1.00 mmol) in acetic acid (30 mL) and $CHCl_3$ (30 mL) were stirred at 80 °C for 24 h under an argon atmosphere. After being cooled to room temperature, the mixture was poured into water, and the resulting solids were collected by filtration. The crude product was purified by column chromatography (PE/DCM = 1:3) to give compound **1b** as a purple solid (0.372 g, 77%). ^{1}H NMR (300 MHz, $CDCl_3$) δ (ppm): 8.83 (s, 2H), 7.64(d, 4H, J = 8.4 Hz), 7.23 (s, 2H), 7.17−7.08 (m, 14H), 6.97(d, 4H, J = 8.7 Hz), 6.70(d, 4H, J = 8.7 Hz), 6.65(d, 4H, J = 8.7 Hz), 3.75(d, 12H, J = 0.9 Hz). ^{13}C NMR (100 MHz, $C_2D_2Cl_4$, 393K) δ (ppm): 160.04, 154.49, 146.71, 145.61, 145.36, 142.53, 140.96, 139.72, 138.05, 134.22, 133.89, 133.82, 133.51, 133.06, 132.78, 132.65, 131.63, 131.02, 129.09, 127.48, 115.09, 114.95, 56.76. HRMS (MALDI, m/z): $(M)^+$ calcd for $C_{64}H_{48}N_4O_4S$, 968.33959; found, 968.33942.

*4,8-Bis[4-(1,2,2-triphenylvinyl)phenyl]benzo[1,2-c:4,5-c′]bis-[1,2,5]thiadiazole (**2a**).* TPE-BTNH (0.414 g, 0.50 mmol), N-sulfinylaniline (0.143 g, 1.00 mmol) and chlorotrimethylsilane (0.100 g, 0.95 mmol) in dried pyridine (30 mL) were stirred at 30 °C for 6 h under an argon atmosphere. After being cooled to the room temperature, the mixture was poured into water and the resulting solids were collected by filtration. The crude product was purified by column chromatography (DCM) to give compound **2a** as a blue solid (0.247 g, 58%). ^{1}H NMR (300 MHz, $CDCl_3$) δ (ppm): 8.05 (d, 4H, J = 8.1 Hz), 7.30−7.27 (m, 4H), 7.17−7.05 (m, 30H). ^{13}C NMR (100 MHz, $C_2D_2Cl_4$, 393K) δ (ppm): 154.42, 145.47, 145.13, 145.01, 143.51, 142.26, 134.75, 132.84, 132.72, 132.62, 132.57, 132.24, 129.17, 129.12, 128.96, 127.95, 127.84, 127.77, 122.46. HRMS (MALDI, m/z): $(M)^+$ calcd for $C_{58}H_{38}N_4S_2$, 854.25377; found, 854.25342.

*4,8-Bis{4-[2,2-bis(4-methoxyphenyl)-1-phenylvinyl]phenyl}benzo-[1,2-c:4,5-c′]bis[1,2,5]thiadiazole (**2b**).* MTPE-BTNH (0.474 g, 0.50 mmol), N-sulfinylaniline (0.143 g, 1.00 mmol) and chlorotrimethylsilane (0.100 g, 0.95 mmol) in dried pyridine (30 mL) were stirred at 80 °C for 24 h under an argon atmosphere. After being cooled to the room temperature, the mixture was poured into water, and the resulting solids were collected by filtration. The crude product was purified by column chromatography (DCM) to give compound **2b** as a green solid (0.358 g, 73%). Because of the limited solubility of **2b** in the NMR solvent, taking the ^{13}C NMR spectrum of **2b** was not possible, even in $C_2D_2Cl_4$ at 393 K. ^{1}H NMR (300 MHz, $CDCl_3$) δ (ppm): 8.06 (d, 2H, J = 8.7 Hz), 7.33−7.29 (m, 4H), 7.19−7.07 (m, 14H), 7.00−6.93 (m, 6H), 6.71−6.64 (m, 8H), 3.76 (t, 12H, J = 6.0 Hz). HRMS (MALDI, m/z): $(M)^+$ calcd for $C_{62}H_{46}N_4O_4S_2$, 974.29601; found, 974.29694.

RESULTS AND DISSCUSSION

Design and Synthesis. To design the AIEE NIR fluorophores suitable for use in OLED by vapor deposition, we selected [1,2,5]thiadiazolo[3,4-g]quinoxaline (QTD) and benzo[1,2-c;4,5-c′]bis[1,2,5]thiadiazole (BBTD) as electron acceptors and tetraphenylethene (TPE) and 2,2-bis(4-methoxyphenyl)-1-phenylethene (MTPE) as both electron donors and

Table 1. Characterizations of Compounds 1a,b and 2a,b

	λ_{abs}^{max} (nm)[a]		λ_{PL}^{max} (nm)[a,b]		Φ_f (%)[c]					
cmpd	soln	film	soln	film	soln	agg.	T_d (°C)[d]	HOMO (eV)[e]	LUMO (eV)[e]	E_g (eV)[f]
1a	518	532	700	704	10.1	36.9	480	−5.39	−3.54	1.85
1b	534	544	780	761	0.28	8.20	454	−5.21	−3.53	1.68
2a	612	635	787	803	13.0	0.26	443	−5.38	−3.71	1.67
2b	632	658	857	883	0.20	6.39	418	−5.22	−3.72	1.50

[a]Solution: measured in THF with a concentration of 1×10^{-5} M. Film: spin-coated on quartz plate. [b]Excitation wavelengths for the emission measurements are equal to their maximum absorption wavelengths. [c]Fluorescence quantum yield (Φ_f) was measured relative to IR-125 (13% in DMSO). Corrections due to the change in solvent refractive indices were applied. Aggregation was measured in a water−THF mixture with 95 vol % water. [d]The onset temperature for 5% weight loss in nitrogen. [e]Calculated from the formula, $E(\text{HOMO}) = -(E_{ox} + 4.34)$ (eV), $E(\text{LUMO}) = -(E_{red} + 4.34)$ (eV). [f]The HOMO−LUMO energy gap (E_g) is derived from the HOMO subtracting LUMO.

AIEE-enabling units. Accordingly, four compounds **1a,b** and **2a,b** (Scheme 1) were designed and expected to have a low HOMO−LUMO gap due to the presence of strong electron-withdrawing acceptors of QTD and BBTD.[48,49] The key step in the entire synthetic route involves the Stille cross-coupling reaction of 4,7-dibromo-5,6-dinitrobenzo[c][1,2,5]thiadiazole with the corresponding tributyltin compounds derived from TPE and MTPE. Reduction of the nitro groups and subsequent cyclization with 1,4-dioxane-2,3-diol or PhNSO furnished the construction of the acceptor moieties of QTD and BBTD, respectively. All the compounds are relatively more soluble in dichloromethane and chloroform than in other common organic solvents. The solubility of **1a,b** and **2a** in chloroform is more than 10 mg/mL at room temperature, while **2b** has a relatively lower solubility of about 2 mg/mL at room temperature. TGA indicates that they are thermally stable and suitable for vapor deposition in OLED device fabrication, as the onset temperatures for 5% weight loss (T_d) in nitrogen range from 418 to 480 °C (Figure S1, Support Information).

Optical Properties. Photophysical properties of these four compounds are summarized in Table 1. The absorption bands from 300 to 450 nm are attributed to $\pi-\pi^*$ and $n-\pi^*$ transitions of the conjugated aromatic segments, and those at longer wavelengths are due to the intramolecular charge transfer between the donors and acceptors (Figure 1). As expected, the use of a stronger donor (e.g., MTPE) or a stronger acceptor (e.g., BBTD) led to a bathochromic shift of the long-wavelength peaks in the absorption and emission spectra. Among all the four compounds, compound **2b** exhibits the longest absorption and emission centered at 658 and 883 nm (with tailing above 1000 nm) in the solid state, respectively (Figure 1 and Table 1). A larger bathochromic shift in photoluminescence observed for **2a** and **2b** as thin films rather than in solution is an indication of more aggregation in the solid state brought by the rigid and polar BBTD acceptor. Accordingly, the NIR emission above 900 nm can be expected by introduction of stronger donors in the BBTD-containing fluorophores.

The AIEE property of these compounds was revealed by comparison of the PL intensity in a water−THF mixture with different water fractions (Table 1 and Figure 2). By a gradual increase of the amount of a nonsolvent of water in the THF solution of these fluorophores, the molecular aggregation occurs, which leads to the changes in PL intensity. In THF solution, compounds **1a** and **2a** are more fluorescent than **1b** and **2b**, while the emission enhancement of the latter pair is relatively more significant than the former pair. The additional bond rotations brought by the four methoxy groups in **1b** and **2b** seem to be responsible for the nonradiative deactivation of

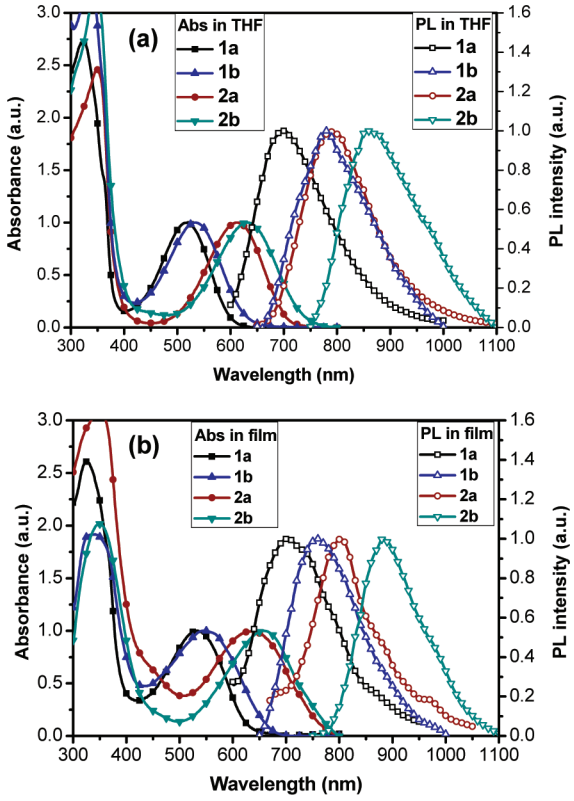

Figure 1. (a) Absorption and PL spectra of compounds **1a,b** and **2a,b** in THF. (b) Absorption and PL spectra of compounds **1a,b** and **2a,b** as thin films.

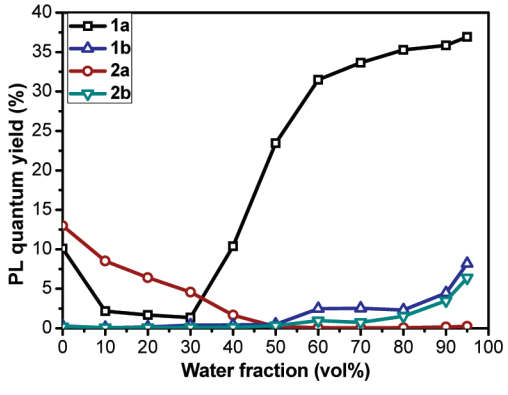

Figure 2. PL quantum yields of compounds **1a,b** and **2a,b** in a water−THF mixture (10 μM) relative to a different fraction of water.

dx.doi.org/10.1021/cm3008733 | *Chem. Mater.* 2012, 24, 2178−2185

the excitons, resulting in the observed low fluorescence in solution.[46] To quantitatively estimate the aggregation-induced emission process, the PL quantum yields were calculated for the compounds in the water−THF mixtures with different water fractions using IR-125 (Φ = 0.13 in DMSO) as the reference (Figure 2). The highly aggregated PL quantum yield of **1a** is attributed to the AIEE effect caused by cross-stacking of propeller-like TPE groups when forming molecular aggregates, in which the suppression of $\pi-\pi$ stacking interaction and the restriction of intramolecular rotations lead to enhancement of fluorescence intensity. Surprisingly, compound **2a** did not show the AIEE, probably because the stronger donor−acceptor system of **2a** is easy to aggregate in a more polar solvent such as water, and the more planar conformation of **2a**, without the methoxy group, leads to more aggregation-caused emission quenching. The photoluminescence of **1a**, **1b**, and **2b** was significantly enhanced in solution upon addition of water. At 95% water fraction, the PL quantum yield of **1a** jumped to 36.9% and the PL quantum yields of **1b** and **2b** increased more than 30 times relative to those in pure THF solution. The PL enhancement is attributed to the AIEE effect caused by the formation of molecular aggregates, in which the suppression of $\pi-\pi$ stacking interaction and the restriction of intramolecular rotations lead to enhancement of fluorescence intensity. Due to the lack of a required instrument, the solid-state quantum yield is difficult to determine accurately. Since the fluorescence quantum yield is proportional to the emission intensity and inversely proportional to the absorption intensity, from the absorption and emission intensity of films with similar thickness (Figure S2, Support Information), it can be estimated that compound **2a** has a relatively higher solid-state quantum yield, which higher than **1b** and **2b** but lower than **1a**. Thus, the AIEE effect of **2a** is weaker than that of **1a**, and it is suppressed when in a polar environment.

Electrochemical Properties. The electrochemical properties of compounds **1a,b** and **2a,b** were investigated by cyclic voltammetry in 0.1 M solution of $(Bu_4N)PF_6$ in dry dichloromethane under argon atmosphere. As shown in Figure 3, they are electrochemically active and undergo the reversible redox reaction. With the methoxy substituents in **1b** and **2b**, an additional oxidation peak is shown at a lower potential and is due to the oxidation of the methoxy group. From the onset of oxidation/reduction potentials, the HOMO, LUMO, and HOMO−LUMO gap levels of these compounds were calculated (Table 1). Compounds **1a** and **2a** have the similar HOMO levels (−5.39 eV and −5.38 eV), as they have the same TPE donor, while the HOMO levels of **1b** and **2b** with the MTPE group are slightly higher (−5.21 eV and −5.22 eV). Similarly, the LUMO energy levels of compounds **2a** and **2b**, with the stronger acceptor of BBTD (−3.71 eV and −3.72 eV), are lower than those of **1a** and **1b** (−3.54 eV and −3.53 eV). Among all, compound **2b** has the lowest HOMO−LUMO gap of 1.50 eV.

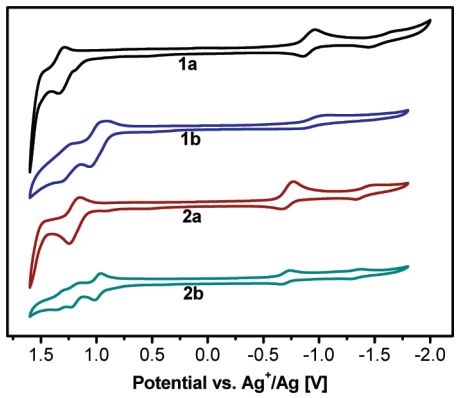

Figure 3. Cyclic voltammograms of compounds **1a,b** and **2a,b** in dichloromethane containing 0.1 M $TBAPF_6$ (scan rate = 50 mV s^{-1}; concentration = 1 × 10^{-3} M).

Electroluminescent Property. Given the enhanced PL property and good processability, all the four compounds were further evaluated as emitters in OLEDs using the following device configuration: ITO/MoO_3(8 nm)/NPB(40 nm)/emitter(20 nm)/TPBi(10 nm)/Alq_3(30 nm)/LiF(1 nm)/Al (100 nm). N,N-Bis(1-naphtyl)-N,N′-diphenyl-1,1,1′-biphenyl-4,4′-diamine (NPB) is chosen for hole-transporting and electron-blocking, and tris(8-hydroxyquinolinato) aluminum (Alq_3) is a typical electron-transporting material. 1,3,5-Tris(N-phenylbenzimidazol-2-yl)benzene (TPBi) is used as the hole-blocking layer, in order to eliminate the visible emission from Alq_3. LiF on the Al cathode and MoO_3 on the ITO anode are used to aid the electron injection and hole injection, respectively. According to the energy diagram of these devices (Figure 4a), the energy level of the emission layer falls between those of NPB and TPBi. Since the carriers are expected to be completely trapped in the emission layer, there should be no emission from NPB and Alq_3, and the device should give exclusively NIR emission from the emitter. Indeed, a single EL peak at above 700 nm was observed in all non-doped devices (Figure 4b). A good match between the EL and PL spectra of these compounds indicates that the observed EL comes solely from the emitter layer due to the blocking layers used in OLEDs. By comparing the device characteristics (Table 2 and Figure 4), one can see a correlation or trade-off between the emission wavelength and device performance. The non-doped device with compound **1a** emits the light with a maximal peak at the shortest wavelength of 706 nm and shows the best performance among all, with the highest radiance of 2917 mW Sr^{-1} m^{-2} at 14 V and a maximum EQE of 0.89% at a current density of 100 mA cm^{-2}. In comparison, the device based on compound **2b** gives the EL peak at the longest wavelength of 864 nm with a lower turn-on voltage (4.4 V) but exhibits a lower EQE (0.20%) at a current density of 100 mA cm^{-2}. The non-doped devices using compounds **1b** and **2a** displayed the EL spectra with a maximum at 749 and 802 nm and the EQE of 0.29% and 0.43% at a current density of 100 mA cm^{-2}, respectively. The relatively low EQE for the non-doped OLEDs based on **1b** and **2b** is mainly due to the low fluorescence quantum yield in the solid state, in addition to the longer emission wavelengths, which lead to the lower photon energy. It is worth noting that the EQE of these devices remained fairly constant over a range of current density of 100−300 mA cm^{-2} (Figure 4d). The result implies that the current-induced fluorescence quenching is effectively suppressed in these devices which should due to the nonplanar structure in solid state of TPE group. The stability and very little efficiency roll-off of these devices as current density increase are suitable for applications requiring high NIR light radiance under high current density.

To demonstrate the benefit of using the AIEE fluorophores in NIR OLEDs, we fabricated the OLEDs using **1a** and **2a** as a dopant in the device configuration of ITO/MoO_3(8 nm)/NPB(40 nm)/Alq_3:dopant emitter(wt%)(20 nm)/TPBi(10

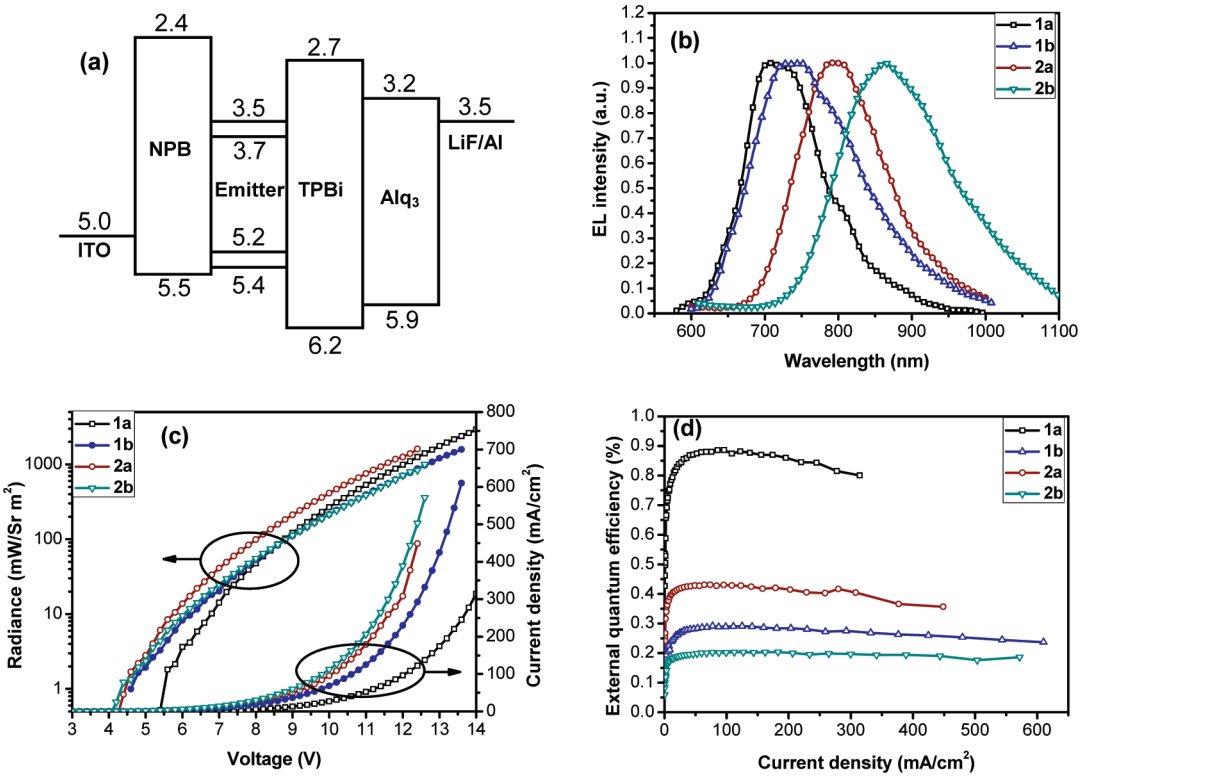

Figure 4. (a) Energy diagram of the devices based on compounds **1a,b** and **2a,b** (relative to the vacuum energy level). (b) Normalized NIR electroluminescence spectra of non-doped devices. (c) Voltage–current density–radiance (V–J–R) characteristics of the non-doped devices. (d) EQE–J characteristics of the non-doped devices.

Table 2. Electroluminescent Data of Non-Doped OLED Devices Using Compounds 1a,b and 2a,b

	V_{on} (V)[a]	λ_{EL}^{max} (nm)	R_{max} (mW Sr^{-1} m^{-2})	η_{ext}^{max} (%)[b]
1a	5.5	706	2917	0.89(0.81)
1b	4.6	749	1576	0.29(0.27)
2a	4.5	802	1604	0.43(0.41)
2b	4.4	864	1003	0.20(0.20)

[a] V_{on} is onset voltage obtained at 1 mW Sr^{-1} m^{-2}. [b] Values in the parentheses taken at a current density of 300 mA cm^{-2}[n].

nm)/Alq_3(30 nm)/LiF(1 nm)/Al(100 nm). The doping concentration in Alq_3 as a host was set at 2%, 4%, and 8%. Figure 5 shows the EL spectra in visible region of the devices with different dopant concentration. At a low doping concentration (2%), the devices based on **1a** and **2a** emitted the visible and NIR light. The visible emission at 535 nm comes from the host Alq_3 as a result of incomplete energy transfer from the host to the dopant (**1a** or **2a**). As the doping concentration increased, the visible EL peak diminished and completely disappeared when the 8% dopant was used. The voltage–current density–radiance (V–J–R) characteristics of these doped devices are shown in Figure S3 (Support Information). In comparison with the non-doped OLEDs, the EQE of the doped devices based on **1a** was significantly lower by at least 4 times (Figure 6). The EQE decreases when the **1a** doping concentration increased to 8% because the energy transfer from Alq_3 was more inefficient in high doping concentration and the more nonradiative deactivation from **1a** via intramolecular rotation. The observed higher EQE for

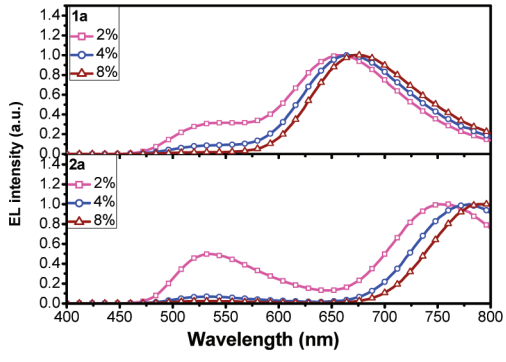

Figure 5. Normalized electroluminescence spectra of doped devices based on compounds **1a** and **2a**.

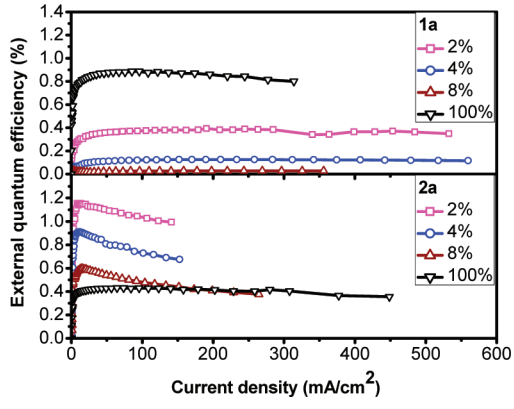

Figure 6. EQE–J characteristics of the doped devices in comparison with non-doped devices based on compounds **1a** and **2a**.

dx.doi.org/10.1021/cm3008733 | Chem. Mater. 2012, 24, 2178–2185

the non-doped OLED is clearly attributed to the AIEE property of compound **1a**. When using compound **2a**, the non-doped device exhibited much lower EQE than the doped devices. A maximal EQE of 1.15% and a radiance of 1523 mW Sr^{-1} m^{-2} at 10.8 V were achieved with a 2% doping concentration. Thus, the EQE of OLEDs based on **2a** increases with the decrease of doping concentration. Compound **2a** can adopt a more rigid and planar conformation as a result of the stronger donor−acceptor structure, which reduces the probability of intramolecular rotation in doped device and thus leads to more aggregation-caused emission quenching in non-doped device. In addition, the EQE of **2a**-doped devices decreased relatively faster with the increase of the current density and were unstable at a high current density.

■ CONCLUSION

In conclusion, a series of structurally simple, thermally stable NIR fluorophores with TPE-enabled aggregation-induced emission enhancement have been prepared. Photoluminescence of these chromophores ranges from 600 to 1100 nm. Non-doped OLEDs utilizing them as emitters are fabricated, which give NIR emission above 700 nm in high efficiencies and a maximum EQE of 0.89%, and which remained fairly constant over a range of current density of 100−300 mA cm^{-2}, have been achieved. A contrast between non-doped and doped OLEDs with these materials confirms that AIEE compounds are suitable for fabricate efficient and stable nondoped NIR OLEDs.

■ ASSOCIATED CONTENT

Ⓢ Supporting Information

^{1}H NMR, ^{13}C NMR, and HRMS spectra and TGA traces of **1a,b** and **2a,b**, absorption and PL spectra of films with the actual measured intensity, the VJR characteristics of **1a**-doped and **2a**-doped devices. This material is available free of charge via the Internet at http://pubs.acs.org.

■ AUTHOR INFORMATION

Corresponding Author

*Email: wwjoy@ciac.jl.cn.

Notes

The authors declare no competing financial interest.

■ ACKNOWLEDGMENTS

This work was supported by the Natural Science and Engineering Research Council of Canada and National Natural Science Foundation of China (21134005, 21074132, 20920102032, and 20834001).

■ REFERENCES

(1) Weil, T.; Vosch, T.; Hofkens, J.; Peneva, K.; Müllen, K. *Angew. Chem., Int. Ed.* **2010**, *49*, 9068.
(2) Giepmans, B. N. G.; Adams, S. R.; Ellisman, M. H.; Tsien, R. Y. *Science* **2006**, *312*, 217.
(3) Bwambok, D. K.; Zahab, B. E.; Challa, S. K.; Li, M.; Chandler, L.; Baker, G. A.; Warner, I. M. *ACS Nano* **2009**, *3*, 3854.
(4) Williams, E. L.; Li, J.; Jabbour, G. E. *Appl. Phys. Lett.* **2006**, *89*, 083506.
(5) Qian, G.; Wang, Z. Y. *Chem. Asian J.* **2010**, *5*, 1006.
(6) Fabian, J. *Chem. Rev.* **1992**, *92*, 1197.
(7) He, X.; Wang, K.; Cheng, Z. *Wiley Interdiscip. Rev.: Nanomed. Nanobiotechnol.* **2010**, *2*, 349.
(8) Tessler, N.; Medvedev, V.; Kazes, M.; Kan, S.; Banin, U. *Science* **2002**, *295*, 1506.
(9) Kim, D. Y.; Song, D. W.; Chopra, N.; Somer, P. D.; So, F. *Adv. Mater.* **2010**, *22*, 2260.
(10) Law, K. *Chem. Rev.* **1993**, *93*, 449.
(11) Thomas, S. W., III; Joly, G. D.; Swager, T. M. *Chem. Rev.* **2007**, *107*, 1339.
(12) Grimsdale, A. C.; Chan, K. L.; Martin, R. E.; Jokisz, P. G.; Holmes, A. B. *Chem. Rev.* **2009**, *109*, 897.
(13) Fischer, G. M.; Daltrozzo, E.; Zumbusch, A. *Angew. Chem., Int. Ed.* **2011**, *50*, 1406.
(14) Ulrich, G.; Goeb, S.; Nicola, A. D.; Retailleau, P.; Ziessel, R. *J. Org. Chem.* **2011**, *76*, 4489.
(15) Jenekhe, S. A.; Osaheni, J. A. *Science* **1994**, *265*, 765.
(16) Grabowski, Z. R.; Rotkiewicz, K. *Chem. Rev.* **2003**, *103*, 3899.
(17) Mori, T. *Chem. Rev.* **2004**, *104*, 4947.
(18) Bauer, P.; Wietasch, H.; Lindner, S. M.; Thelakkat, M. *Chem. Mater.* **2007**, *19*, 88.
(19) Sonmez, G.; Meng, H.; Wudl, F. *Chem. Mater.* **2003**, *15*, 4923.
(20) Caspar, J. V.; Kober, E. M.; Sullivan, B. P.; Meyer, T. J. *J. Am. Chem. Soc.* **1982**, *104*, 630.
(21) Fenwick, O.; Sprafke, J. K.; Binas, J.; Kondratuk, D. V.; Stasio, F. D.; Anderson, H. L.; Cacialli, F. *Nano Lett.* **2011**, *11*, 2451.
(22) Ellinger, S.; Graham, K. R.; Shi, P.; Farley, R. T.; Steckler, T. T.; Brookins, R. N.; Taranekar, P.; Mei, J.; Padilha, L. A.; Ensley, T. R.; Hu, H.; Webster, S.; Hagan, D. J.; Stryland, E. W. V.; Schanze, K. S.; Reynolds, J. R. *Chem. Mater.* **2011**, *23*, 3805.
(23) Qian, G.; Zhong, Z.; Luo, M.; Yu, D.; Zhang, Z.; Ma, D.; Wang, Z. Y. *J. Phys. Chem. C* **2009**, *113*, 1589.
(24) Yang, Y.; Farley, R. T.; Steckler, T. T.; Eom, S. H.; Reynolds, J. R.; Schanze, K. S.; Xue, J. *J. Appl. Phys.* **2009**, *106*, 044509.
(25) Ho, C. C.; Chen, H. F.; Ho, Y. C.; Liao, C. T.; Su, H. C.; Wang, K. T. *Phys. Chem. Chem. Phys.* **2011**, *13*, 17729.
(26) Borek, C.; Hanson, K.; Djurovich, P. I.; Thompson, M. E.; Aznavour, K.; Bau, R.; Sun, Y.; Forrest, S. R.; Brooks, J.; Michalski, L.; Brown, J. *Angew. Chem.* **2007**, *119*, 1127.
(27) Sommer, J. R.; Shelton, A. H.; Parthasarathy, A.; Ghiviriga, I.; Reynolds, J. R.; Schanze, K. S. *Chem. Mater.* **2011**, *23*, 5296.
(28) Graham, K. R.; Yang, Y.; Sommer, J. R.; Shelton, A. H.; Schanze, K. S.; Xue, J.; Reynolds, J. R. *Chem. Mater.* **2011**, *23*, 5305.
(29) Baldo, M. A.; O'Brien, D. F.; You, Y.; Shoustikov, A.; Sibley, S.; Thompson, M. E.; Forrost, S. R. *Nature* **1998**, *395*, 151.
(30) Cheng, K. Y.; Anthony, R.; Kortshagen, U. R.; Holmes, R. J. *Nano Lett.* **2010**, *10*, 1154.
(31) Sharbati, M. T.; Rad, M. N. S.; Behrouz, S.; Gharavi, A.; Emami, F. *J. Lumin.* **2011**, *131*, 553.
(32) Qian, G.; Zhong, Z.; Luo, M.; Yu, D.; Zhang, Z.; Wang, Z. Y.; Ma, D. *Adv. Mater.* **2009**, *21*, 111.
(33) Jäkle, F. *Chem. Rev.* **2010**, *110*, 3985.
(34) Zhao, Z.; Chen, S.; Lam, J. W. Y.; Jim, C. K. W.; Chan, C. Y. K.; Wang, Z.; Lu, P.; Deng, C.; Kwok, H. S.; Ma, Y.; Tang, B. Z. *J. Phys. Chem. C* **2010**, *114*, 7963.
(35) Hong, Y.; Lam, J. W. Y.; Tang, B. Z. *Chem. Commun.* **2009**, 4332.
(36) Qin, A.; Lam, J. W. Y.; Tang, L.; Jim, C. K. W.; Zhao, H.; Sun, J.; Tang, B. Z. *Macromolecules* **2009**, *42*, 1421.
(37) Kokado, K.; Chujo, Y. *Macromolecules* **2009**, *42*, 1418.
(38) Tang, W.; Xiang, Y.; Tong, A. *J. Org. Chem.* **2009**, *74*, 2163.
(39) Yuan, W. Z.; Lu, P.; Chen, S.; Lam, J. W. Y.; Wang, Z.; Liu, Y.; Kwok, H. S.; Ma, Y.; Tang, B. Z. *Adv. Mater.* **2010**, *22*, 2159.
(40) Zhang, X.; Chi, Z.; Li, H.; Xu, B.; Li, X.; Liu, S.; Zhang, Y.; Xu, J. *J. Mater. Chem.* **2011**, *21*, 1788.
(41) Zhao, Z.; Chen, S.; Lam, J. W. Y.; Lu, P.; Zhong, Y.; Wong, K. S.; Kwok, H. S.; Tang, B. Z. *Chem. Commun.* **2010**, *46*, 2221.
(42) Thomas, K. R. J.; Lin, J. T.; Velusamy, M.; Tao, Y. T.; Chuen, C. H. *Adv. Funct. Mater.* **2004**, *14*, 83.
(43) Qian, G.; Dai, B.; Luo, M.; Yu, D.; Zhan, J.; Zhang, Z.; Ma, D.; Wang, Z. Y. *Chem. Mater.* **2008**, *20*, 6208.

(44) Uno, T.; Takagi, K.; Tomoeda, M. *Chem. Pharm. Bull.* **1980**, *28*, 1909.
(45) Banerjee, M.; Emond, S. J.; Lindeman, S. V.; Rathore, R. *J. Org. Chem.* **2007**, *72*, 8054.
(46) Benson, R. C.; Kues, H. A. *J. Chem. Eng. Data* **1977**, *22*, 379.
(47) Greenham, N. C.; Friend, R. H.; Bradley, D. D. C. *Adv. Mater.* **1994**, *6*, 491.
(48) Bundgaard, E.; Krebs, F. C. *Macromolecules* **2006**, *39*, 2823.
(49) Susumu, K.; Duncan, T. V.; Therien, M. J. *J. Am. Chem. Soc.* **2005**, *127*, 5186.
(50) Hong, Y.; Lam, J. W. Y.; Tang, B. Z. *Chem. Soc. Rev.* **2011**, *40*, 5361.